Acta Biochim Biophys Sin (2010): 266–273 | © The Author 2010. Published by ABBS Editorial Office in association with Oxford University Press on behalf of the Institute of Biochemistry and Cell Biology, Shanghai Institutes for Biological Sciences, Chinese Academy of Sciences. DOI: 10.1093/abbs/gmq014.
Advance Access Publication 1 March 2010

Original Article

Tandem affinity purification and identification of the human TSC1 protein complex

Longhua Guo[1], Wantao Ying[1], Jiyang Zhang[1], Yanzhi Yuan[1], Xiaohong Qian[1], Jian Wang[1*], Xiaoming Yang[1*], and Fuchu He[1,2*]

[1]State Key Laboratory of Proteomics, Beijing Proteome Research Center, Beijing Institute of Radiation Medicine, Beijing 102206, China
[2]Institutes of Biomedical Sciences, Fudan University, Shanghai 200032, China
*Correspondence address. Tel: +86-10-68177417; E-mail: hefc@nic.bmi.ac.cn (F.H.). Tel: +86-10-66931424; E-mail: xmyang2@nic.bmi.ac.cn (X.Y.). Tel: +86-10-80705118; E-mail: wangjian@nic.bmi.ac.cn (J.W.)

Mutations in the *TSC1* and *TSC2* genes lead to tuberous sclerosis complex (TSC), which is characterized clinically by mental retardation, epilepsy, and benign tumors affecting multiple tissues. Numerous components of the TSC protein complex remain uncharacterized. Here we report the purification of the TSC1 complex under physiological conditions using a proteomic strategy. We purified the TSC1 protein complex using a tandem affinity purification method and identified a protein complex containing 139 components. Two known binding proteins of TSC1 (TSC2 and DOCK7) were identified along with other new potential partners, which cover reported and novel TSC1 functional categories. Bioinformatics and biochemical methods were used to evaluate the observed protein–protein interactions. A comparative analysis with a published expression proteomics/genomics study of TSC1 revealed more than 20 common candidates that might be functionally relevant. The data set provides new directions in which to expand our knowledge of the functions of TSC1 and the mechanisms of TSC. The results are highly reliable, which is reflected by the identification of a few reported partners of TSC1 and many TSC1/2-regulated proteins. Interestingly, many new functional categories were identified, such as DNA repair, which provide novel hints to the function of TSC1. Moreover, a few neuronal disease-related proteins that might regulate the normal functions of neurons were identified. Thus, the results suggest that many of the new interactions should be biologically significance. It will be interesting to further investigate the regulatory mechanisms of these components.

Keywords TSC1; tandem affinity purification; proteomics

Received: August 19, 2009 Accepted: January 18, 2010

Introduction

Tuberous sclerosis complex (TSC) is an autosomal dominant disorder characterized by the widespread development of distinctive tumors, called hamartomas, in a variety of tissues, such as eyes, skin, kidney and brain, which can be caused by mutation of either the *TSC1* or the *TSC2* gene [1]. TSC1 and TSC2 have been confirmed to form a complex *in vivo*, providing an explanation for the similar disease phenotypes caused by mutation of either TSC1 or TSC2 [2,3], and TSC1 is usually considered to function in a similar pathway with TSC2, which has been extensively studied. However, unique functions of TSC1 and TSC2 in different cell compartments have been implied [4,5]. Another unknown component of the TSC1/TSC2 complex has also been suggested [3]. Recent discoveries of new phosphorylation sites on TSC1 have also raised the question of how TSC1 is regulated [6,7]. A proteomics study of TSC1-binding proteins may provide useful clues to help investigate these problems and provide a clearer picture of TSC1 function, especially in the protein complex, which more closely reflects the physiological entity of the proteins in the cell [8,9].

Several genomics and proteomics studies focusing on TSC2 have been conducted [10–16], whereas studies on TSC1 have been mainly reported by Hengstschlager's group. Genes and proteins in HeLa cells deregulated by overexpression of TSC1 were analyzed by cDNA microarray and 2-dimensional (2-D) gel electrophoresis with subsequent mass spectrometry identification [12–16]. These approaches all provided new insights into the cellular roles of TSC proteins.

Here, we report the purification of the human TSC1 complex taking advantage of the tandem affinity purification (TAP) method [17–19]. The sequential use of two affinity tags reduces the background of nonspecific-binding proteins, and the mild buffer conditions preserve weak

protein–protein interactions. By retrovirus-mediated gene transfer, we expressed the tagged TSC1 protein at close to the endogenous level so that we could study the functions of TSC1 under physiological conditions. With this TAP-MS/MS approach, 139 proteins that potentially associate with TSC1 were identified. Selected protein–protein interactions were further validated. Our study reveals the complexity of the TSC1 complex and uncovers multiple previously unknown binding partners of TSC1. It provides a basis for further investigation of the biological functions and molecular mechanisms of the TSC complex.

Materials and Methods

Plasmids

The human *TSC1* cDNA was a kind gift from Dr Kunliang Guan (University of MI, USA). Basically, the *TSC1* gene was amplified by PCR using pcDNA3-Myc3-hTSC1 as the template. Then the product was inserted into the *Eco*RI site of the TAP plasmid pZome-1-N (EUROSCARF, University of Frankfurt, Germany). The correct orientation and sequence of the insert in pZome1N-TSC1 was confirmed by sequencing.

Cell culture, retrovirus packaging, and stable cell line selection

Human hepatocellular carcinoma HepG2 cells and human embryonic kidney (HEK) 293T cells (Peking Union Medical College, Beijing, China) were cultured in Dulbecco's modified Eagle's medium supplemented with high glucose (Gibco, Grand Island, USA) and 10% fetal bovine serum. Retroviruses were packaged with pZome1N-TSC1 or pZome1N as described [20]. HepG2 cells expressing TAP-tagged TSC1 or TAP tag were selected by the addition of 2 μg/ml puromycin (Sigma, St. Louis, USA) to the medium 48 h after retroviruses infection. Stable cell lines were collected for storage or large-scale culture. Large-scale cell culture was carried out in Cell Factories (NUNC, Roskilde, Denmark).

Co-immunoprecipitation assay

HEK293T cells were transfected with the indicated plasmids using Lipofectamine™ 2000 (Invitrogen, Carlsbad, USA). After 48 h, the cells were harvested and lysed with 1 ml of IPP150 containing 10 mM Tris–HCl (pH 8.0), 150 mM NaCl, 0.5% NP-40 (Sigma), 1 mM DTT supplemented with protease (Complete Mini EDTA-free; Roche Applied Science, Indianapolis, USA), and phosphatase inhibitors (2 mM sodium orthovanadate, 1 mM NaF) on ice for 30 min. Immunoprecipitation assays were performed using anti-c-Myc (9E10) (Santa Cruz Biotechnology, Santa Cruz, USA) or anti-Flag M2 (Sigma) antibodies. The washing steps were performed three times with IPP150 for each of the immunoprecipitation assay. Lysates and immunoprecipitates were analyzed using the indicated primary antibodies and then the appropriate secondary antibody, followed by detection with an ECL western blotting substrate (Pierce, Rockford, USA).

Tandem affinity purification

All procedures were carried out as described at 4°C with some modifications [2,3]. Approximately 1×10^9 HepG2 cells were used. The cells were lysed with 30 ml of IPP150 (0.5% NP-40) supplemented with protease inhibitors (Complete Mini EDTA-free, Roche Applied Science) and phosphatase inhibitors (2 mM sodium orthovanadate and 1 mM NaF) on ice for 30 min. Samples were cleared by centrifugation at 20,000 *g* for 15 min. The supernatant was transferred to 50-ml tubes (Corning, New York, USA). Pellets were frozen in liquid nitrogen, thawed at room temperature three times, centrifuged at 20,000 *g* for 10 min, and combined with the first supernatant. Then the whole cell lysates were incubated with 150 μl of IgG beads for 2 h. Beads were transferred to a 10-ml empty ploy-prep chromatography column (Bio-Rad, Hercules, USA) and washed extensively with 30 ml of IPP150 (0.1% NP-40) and then with 15 ml of TEV cleavage buffer (10 mM Tris–HCl, pH 8.0, 150 mM NaCl, 0.1% NP-40, 0.5 mM EDTA, and 1.0 mM DTT). TEV cleavage was performed in 1 ml of TEV cleavage buffer with 150 U of TEV protease (Invitrogen) at 16°C. After 2 h, the cleavage solution was transferred into another ploy-prep column containing 150 μl of equilibrated calmodulin affinity resin (Stratagene, La Jolla, USA) and rotated for 2 h. Thirty milliliters of calmodulin-binding buffer (10 mM Tris–HCl, pH 8.0, 150 mM NaCl, 0.1% NP-40, 1 mM magnesium acetate, 1 mM imidazole, 2 mM $CaCl_2$, and 10 mM β-mercaptoethanol) was used to wash the resin. Finally, proteins were eluted with calmodulin elution buffer (10 mM Tris–HCl, pH 8.0, 150 mM NaCl, 0.1% NP-40, 1 mM magnesium acetate, 1 mM imidazole, 10 mM β-mercaptoethanol, and 20 mM EGTA) (200 μl of each for six fractions). Eluates were precipitated by the TCA method [18].

Protein digestion

Precipitated proteins from pZome1N-TSC1 and pZome1N strains were dissolved in SDS loading buffer, separated by 10% SDS-PAGE and stained with Coomassie Brilliant Blue R250 in parallel. After image scanning and documentation, the gel slices that showed differences were selectively excised for identification. For trypsin digestion, gel slices were cut into cubes, destained with 50% acetonitrile containing 25 mM NH_4HCO_3 and subjected to reduction and alkylation. Then the gel plugs were lyophilized and immersed in 15 μl of 10 ng/μl trypsin solution in 25 mM NH_4HCO_3. The digestion was incubated at 37°C for 15 h. Peptide mixtures were first extracted with 100 μl of 5% TFA at 40°C for

1 h and then 2.5% trifluoroacetic acid/50% acetonitrile at 30°C for 1 h. The extracted solutions were combined, lyophilized, and prepared for the following analysis.

Nano-RPLC-MS/MS identification

Lyophilized tryptic peptides were subjected to Nano-RPLC-MS/MS using a Thermo Finnigan linear ion trap mass spectrometer (LTQ) (Thermo Finnigan, San Jose, USA) equipped with an NSI source. The initial nanoLC run was performed on a LC packing system configured with Famous, Swithos and Ultimate and controlled by the Dionex chromatography software (Dionex, Sunnyvale, USA). The 10-port valve of the Ultimate system was equipped with two RP-C18 trap columns, which allows for synchronous sample loading and desalting of one trap column whereas the other is eluted to the MS through a PicoFritTM tip analysis column (BioBasic C18, 5 μm, 75 μm i.d. × 10 cm, 15 μm i.d. spray tip; New Objective, Woburn, USA) by an Ultimate pump using a stepwise mobile phase gradient of 2–40% B (80% ACN, 0.1% FA in water) for 30 min and 40–100% B for 5 min. The LTQ-MS was operated under the following parameters: normalized collision energy of 35%, temperature of the ion transfer of 200°C, and spray voltage of 1.8 kV. The mass spectrometer worked under an 'nth order triple play' mode, which repeats the zoom scan and MS/MS acquisition for the five most intense ions following one full MS scan using the following dynamic exclusion settings: repeat count of 2, repeat duration of 30 s, exclusion list size of 150, and exclusion duration of 90 s. Under the zoom scan mode, we obtained a spectrum with resolution good enough for the discrimination of different charge states, so that singly charged ions, most of which come from contaminants, could be excluded and only ions with charges of 2 or greater could be considered for further MS/MS analysis.

Domain analysis

The Simple Modular Architecture Research Tool (SMART; http://smart.embl.de) was used for protein domain identification and analysis of protein domain architecture. As a comparable background, 150 of proteins were selected randomly from the IPI human proteins database version, 3.07 (50,207 protein sequences) for 100, 200, 500, 1000, 2000, 5000, 10,000, 20,000, and 30,000 times, respectively. Sequences of these proteins were extracted and submitted to SMART. No bias will exist if the conclusion is drawn from the distribution of the 10,000 sample points. The hypergeometric cumulative distribution function was used to evaluate the probability of zero to 45 proteins containing coiled-coil domains in every 150 proteins selected randomly from 22,972 proteins, which includes 2650 proteins containing coiled-coil domains. The 22,972 proteins have predicted domain structures by SMART analysis based on the IPI human protein database 3.07.

Functional annotation

The functional annotation and classification of the data set was based on gene ontology (biological process and cellular component; http://www.geneontology.org) and published papers. The OMIM web-based tool (Online Mendelian Inheritance in Man; http://www.ncbi.nlm.nih.gov/omim) was used for disease phenotype analysis.

Results

TAP and identification of the TSC1 protein complex

Retrovirus-mediated gene transfer was used to express TAP-tagged TSC1 at a near-endogenous level in HepG2 cells (**Fig. 1**). We believe that the false positives caused by overexpression were greatly reduced. First, from experiences of previous research, the non-physiological complexes caused by overexpression can be reduced by lowering the expression level of the target protein [17]. Second, we had used an overexpression method (unpublished data) to purify the TSC1 complex and no reported interactions were found. In contrast, few known partners of TSC1 were identified in the current study (such as TSC2). Basically, the tagged *TSC1* gene was stably inserted into the mammalian cell genome by retrovirus infection. The expression level of tagged TSC1 was modified to close to the endogenous level by changing the multiplicity of infection. Cells stably expressing the TAP tag only were generated in the same way and used as a purification control. TAP procedures were carried out as described at 4°C with some modifications [17,18]. The purification was carried out two times with approximately 1×10^9 cells. TSC2 was recovered as an interaction partner, indicating that the purifications worked. The eluates were precipitated with the TCA method, separated by 10% SDS-PAGE, and visualized by Coomassie Brilliant Blue R250 staining (**Fig. 2**).

For MS/MS identification, bands specific to the TAP-TSC1 sample were excised and digested with trypsin. Lyophilized tryptic peptides were subjected to Nano-RPLC-MS/MS analysis. All MS/MS spectra were

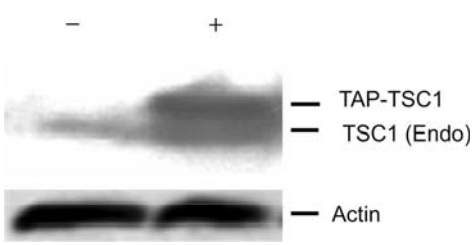

Figure 1 Expression level of TAP-tagged TSC1 in HepG2 cells Equal amounts of cell extracts from HepG2-TAP-TSC1 (+) and HepG2-TAP (−) stable cell lines were subjected to SDS-PAGE and analyzed with anti-TSC1 or anti-actin antibodies as indicated. The band in the HepG2-TAP cell extract indicates the position of endogenous TSC1 (Endo, top panel).

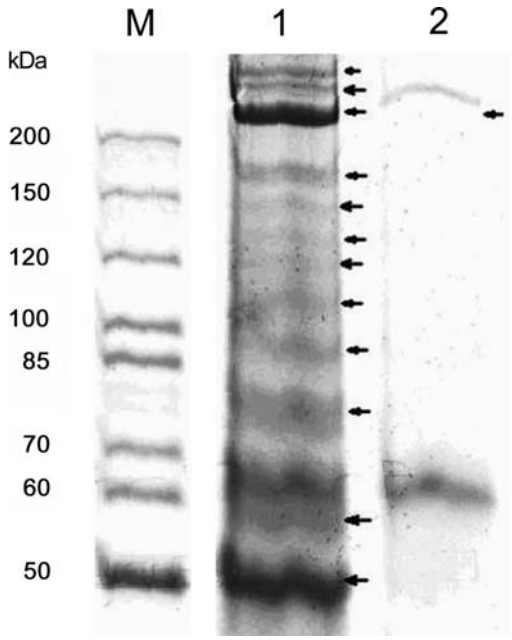

Figure 2 SDS-PAGE analyses of purified TSC1-associated proteins Equal amounts of HepG2-TAP-TSC1 and HepG2-TAP cells ($\sim 10^9$ cells) were subjected to lysis and purification. After TCA precipitation, the pellet was run on 10% SDS-PAGE. Separated proteins (M, molecular weight marker; lane 1, HepG2-TAP-TSC1 cells; lane 2, HepG2-TAP cells) were visualized by Coomassie blue staining. The positions of the molecular weight markers are indicated. Arrows indicate bands excised for LC-MS/MS analysis. The nonspecific binding bands to TAP-tag (lane 2) were also excised for MS analysis.

searched against the human IPI protein database (version 3.07) using the SEQUEST algorithm in the Bioworks software (version 3.1) for peptide and protein identification. Only a tandem spectrum with more than 15 ions totaling 100 counts was accepted for database searching, whereas the tolerance for peptides during data generation was 1.4 Da and another 2.0 Da was used for database searching. Search results were assembled using the Build Summary software [21] and filtered with the parameters of a ΔCn cutoff value $\geq$0.08 and Xcorr scores of $\geq$2.5 for doubly charged and $\geq$3.5 for triply charged peptides. The nonspecific-binding proteins to TAP tag were excluded from further analyzing, which include actin, eukaryotic translation elongation factor 1 beta 2, heat shock 70 kDa protein 6, and a hypothetical protein (IPI00430808). In total, 12 bands were cut out and analyzed. The peptides from MS identification were corresponding to 139 proteins (**Supplementary Tables S1** and **S2**). The data set might contain few nonspecific-binding partners and should be verified by further research.

Validation of the data set by co-immunoprecipitation assay

To validate the confidence of the TSC1 complex data set, six proteins were randomly selected for co-immunoprecipitation

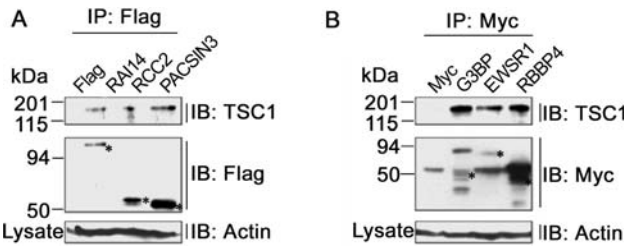

Figure 3 Validation of protein–protein interactions by co-immunoprecipitation The Flag- or Myc-tagged genes were transiently transfected into HEK293T cells. After 48 h, the cell lysates were immunoprecipitated with anti-Flag (A) or anti-Myc (B) antibodies and subjected to western blot with the anti-TSC1 antibody. The empty Flag or Myc vector was used as the negative control. The actin was used as a loading control for the lysates. The target proteins bands were marked with asterisk.

assays. Myc-tagged EWSR1, RBBP4, and G3BP and Flag-tagged PACSIN3, RAI14, and RCC2 were ectopically expressed in human HEK293T cells and subjected to immunoprecipitation. As shown, the anti-TSC1 antibody was used to detect the existence of TSC1 in all six associated complexes [**Fig. 3(A,B)**], which suggests that the data set is reliable. The expression of RBBP4 was reported to be up-regulated as a result of TSC1/TSC2 overexpression [14]. It might be interesting to test whether TSC1 can directly regulate the level of RBBP4. In the data set, two known binding partners of TSC1, TSC2, and DOCK7 [6], were also pulled down. All of the other identified interactions of the TSC1 complex are novel.

Functional classification of the TSC1 complex components

First, we grouped all of the identified proteins according to their biological functions (**Fig. 4** and **Supplementary Table S1**). As expected, proteins involved in the cell cycle, cell adhesion, and cell cytoskeleton organization were enriched, which correlates well with the reported functions of TSC1. In addition, a few new functional categories were identified, such as pre-mRNA splicing, DNA repair, and transcription. Multiple useful hints to the functions or regulatory mechanisms of TSC1 can be found in the data set.

Second, the cellular localizations of proteins that potentially bind to TSC1 were analyzed (**Fig. 4**, right panel). We found that the largest proportion of proteins was localized in intracellular membrane-bound organelles (39%), and a relatively smaller proportion of proteins was localized to the cytoskeleton (19%) and cytoplasm (13%), which is consistent with former studies of TSC1 localization [4,22]. There were also a large proportion of proteins localized in the nucleus (29%). While TSC1 translocation into nucleus from the cytoplasm under normal conditions remains to be determined, a few studies have shown a

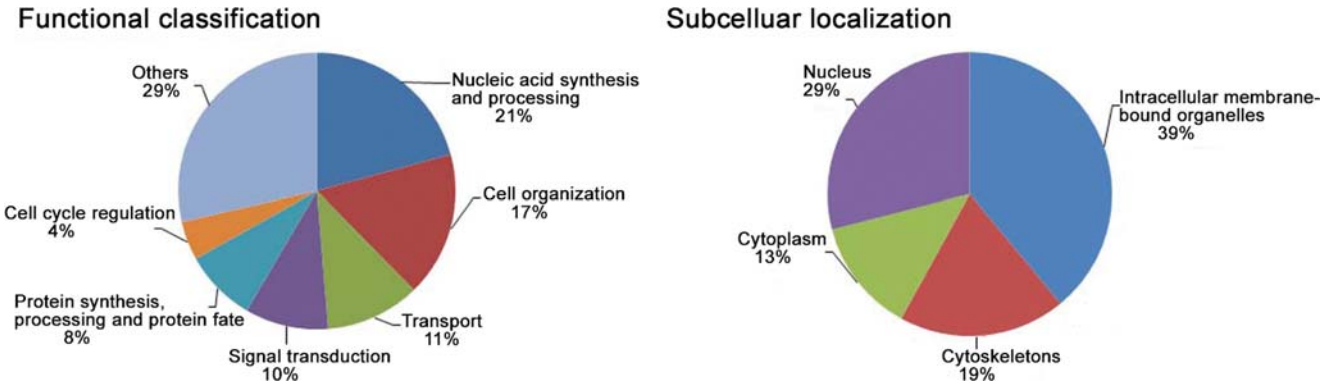

Figure 4 Functional classification and subcellular localization of TSC1 interactors The functional annotations and classifications of the data set were obtained from Gene Ontology (biological process and cellular component) and published papers.

nuclear localization of TSC1 [23,24]. The functions of TSC1 might be diverse with different localizations.

Third, the TSC1 complex data set was subjected to OMIM (Online Mendelian Inheritance in Man, http://www.ncbi.nlm.nih.gov/omim) to analyze the disease phenotypes of the proteins. Twenty-nine proteins are associated with different diseases (**Supplementary Table S3**), such as neurological, metabolic, and developmental diseases and cancer. The results are consistent with the function of TSC1 and provide potential mechanisms of TSC1 in the development of related diseases.

The proteins containing coiled-coil domains are enriched

Domains are basic structural and functional units of proteins, which may mediate protein–protein interactions. We analyzed the domain information of the TSC1 complex using the web-based tool SMART (**Supplementary Table S1**). Interestingly, coiled-coil domains appear with a significantly higher frequency in our protein list compared with the randomly selected 150 proteins from the IPI human proteins database. The frequency of coiled-coil domains in our data set was about 0.57 (85 of coiled-coil domains in 150 proteins), while the random chance is 0.038. Coiled-coil domains in the TSC1 purified proteins were enriched 15 times. Coiled-coil domains mediate protein–protein interactions [25], and it raises the possibility that at least some of the partners might directly associate with TSC1 through a coiled-coil domain.

Comparison of the TSC1 protein complex data set with other proteomics data set

A considerable coincidence was found with a reported microarray and 2-D gel/MS data analysis of TSC1/TSC2 overexpression in cells [10–12,14,16]. For example, when functionally grouped, both data sets show proteins involved in the hexose metabolism and nitrogen compound metabolism (data not shown). Twenty-seven common candidates were found (**Table 1**), such as RBBP4, P4HB, and VIM, etc. EWSR1 and RBBP4 have been confirmed to interact with TSC1 by co-immunoprecipitation assay in HEK293 cells (**Fig. 3**). These results imply that some of the proteins whose expression changes with the TSC overexpression may directly associate with the TSC protein complex either as part of the function of these complexes or to regulate it. Only seven proteins match with the observed size of the protein bands on the gel in **Table 1**. They might be false positives if the proteins cannot match with the observed size on the SDS-PAGE gel. But there are some difficulties to distinguish them with the true positives. First, it is common that a protein does not match its calculated molecular weight [26,27]. For example, more than 40% of proteins did not match to their calculated positions in fission yeast [26]. Second, the molecular weight of a protein is determined by the status of hydrophobicity, charges or post-translational modifications. The predicted methods cannot tell the exact size of a given protein. For example, the glycosylation can make a protein larger than that it appears to be. Third, the sample process or protein degradation may induce unexpected proteolytic cleavage of expressed proteins, which leads to a protein smaller than it should be. Fourth, the alternative splicing of a gene can result in different size of a protein. We still lack all of such information for the human genes. Lastly, according to our knowledge, we cannot find an effectively published method to exclude such kind of false positives.

Discussion

The tumor suppressor TSC1-associated complex formed *in vivo* was purified by TAP tag and analyzed by MS. The reliability of this data set was demonstrated by co-immunoprecipitation assays. A few reported partners of TSC1 and many TSC1/2-regulated proteins were also identified, which indicates that we identified *bona fide* partners of TSC1 and that its function is complex. The identified proteins may include the proteins that interact with TSC2, not

Table 1 Common molecules among the data sets of the TSC1 complex, the microarray, and the 2-D gel/MS data with TSC1/TSC2 overexpression

TAP	Microarray	2-D gel/MS	Gene name	Function	Match[a]
ADD1	ADD1	–	Alpha adducin	Promotes the assembly of the spectrin–actin network	N
ATXN2L	ATXN1	–	Ataxin-2-like protein	Spinocerebellar ataxia	N
CANX	CANX	–	Calnexin precursor	Quality control in ER	N
CORO1C	CORO1A	–	Coronin-1C	Actin-binding, signal transduction, apoptosis, and gene regulation	N
CTNNA1	CTNNA2	–	Alpha E-catenin	Cell differentiation, cancer invasion and metastasis	Y
DLST	DLSTP	–	Dihydrolipoamide *S*-succinyltransferase	Associated with Alzheimer's disease	N
DOCK7	DOCK1	–	Dedicator of cytokinesis protein 7	GEF, no activity for Cdc42	N
EWSR1[b]	EWSR1	–	RNA-binding protein EWS	Aberrant activation of the fusion protein target genes	N
FLNA	FLNA	–	Filamin A	Reorganization of actin cytoskeleton; periventricular nodular heterotopia 1 (neuron migration failure)	Y
GPIAP1	GPIAP1	–	P137gpi	Cell cycle associated protein 1	N
H2-ALPHA	–	H2-ALPHA	Tubulin	Constituent of microtubules	N
JUP	JUP	–	Junction plakoglobin	Catenin	N
MAP4	MAP4	–	Microtubule associated protein 4	Binds CyclinB/Cdc2	Y
MCM6	MCM7	–	DNA replication licensing factor MCM6	DNA replication	N
MTHFD1	MTHFD1	–	C1-THF synthase	Amino acid synthesis	Y
MYH9	MYO5A	–	Myosin heavy chain	Cytokinesis, cell shape	N
P4HB	–	P4HB	Protein disulfide isomerase	Belongs to the protein disulfide isomerase	N
PFKP	PFKP	–	Phosphofructokinase 1	ATP + D-fructose 6-phosphate = ADP + D-fructose 1,6-bisphosphate	Y
PPP2R1A	PPP2R1A	–	PP2A, subunit A, R1-alpha isoform	Scaffolding molecule	N
PSMD2	PSMD13	–	Tumor necrosis factor type 1 receptor associated protein 2	Regulatory subunit of the 26S proteasome, TNF signalling	Y
RBBP4[b]	–	RBBP4	Chromatin assembly factor 1 subunit c	Targeting chromatin assembly factors, chromatin remodeling factors and histone deacetylases to their histone substrates	N
RPS27A	RPS27A	–	40S ribosomal protein S27a	Ribosomal protein	N
SLC3A2	SLC1A3,SLC19A1	–	4F2 cell-surface antigen heavy chain	Binding to integrin, amino acid transport	N
SPTAN1	SPTAN1	–	Spectrin	Organization of the cytoskeleton	Y
STARD7	STARD1	–	START domain containing 7	Steroidogenic acute regulatory protein	N
TJP1	TJP1	–	Tight junction protein ZO-1	Tight junction	N
VIM	–	VIM	Vimentin	Intermediate filament	N

[a]Match between observed and theoretical molecular weight. [b]The confirmed interactors of TSC1 by co-immunoprecipitation in this study. Y, yes; N, no.

TSC1. Many proteins are shown to bind with TSC2, but not TSC1. In our results, we cannot distinguish them. Dozens of proteins have been reported to interact with TSC1 [28]. We identified numerous proteins of TSC1 complex with multiple functions, such as cell cycle, cell adhesion, cell cytoskeleton organizations, and DNA repair, etc. Further research is needed to confirm the interacting proteins and their functions. The potential value of the data set was reflected by functional classification. As expected, the proteins involved in the cell cycle, cell adhesion, and cell cytoskeleton organization were enriched. Interestingly, many new functional categories were identified, such as DNA repair, which provide novel hints to the function of TSC1. For example, the possible role of TSC1/TSC2 in DNA repair has been linked to chromatin assembly factor 1 (CAF1/RBBP4) and proliferating cell nuclear antigen (PCNA) [14]. In our results, besides RBBP4, we also obtained the two subunits of the Ku complex (XRCC5/XRCC6) and a subunit of the PSF/p54 (nrb) complex, NONO. The Ku complex has been reported to bind to DNA ends during non-homologous end joining (NHEJ) of DNA double-strand break repair [29,30]. Recently, the PSF/p54(nrb) complex was reported to strongly stimulate DNA end joining *in vitro*, to bind directly to the RNA substrates of the end joining reaction and to cooperate with Ku to establish a functional pre-ligation complex [31]. The interaction of RBBP4 with TSC1 was also confirmed in the co-immunoprecipitation assay. Hence, we speculate that TSC1 may play a role in the DNA repair process.

A few useful hints regarding the role of TSC1 in the development of diseases were provided through OMIM analysis of the TSC1 complex data set. For example, TSC1 regulates neuronal morphology and differentiation [32,33]. When mutated, several types of the most significant seizures caused by *TSC* gene dysfunction in the TSC patients occur in the neuronal system. Four neuronal disease-related proteins, including TSC2, were identified. TSC1 may cooperate with this group of proteins to maintain normal function of the neuronal system.

We also found that proteins containing coiled-coil domains were likely to directly associate with TSC1. A considerable coincidence was found with a previously reported microarray and 2-D gel/MS data sets. Thus, all of the results suggest that most of the new interactions should be biologically significant. The TSC1 complex data set will be a valuable resource for the research of TSC1 function. It will be interesting to investigate the regulatory mechanisms of these components in the TSC disease development in future research.

Supplementary Data

Supplementary data are available at *ABBS* online.

Acknowledgements

We thank Dr Jane Wu (University of Northwestern, USA) for kind revision, Li Zhang (Fudan University, China) for technical help and Guangxia Gao and Xuemin Guo (Institute of Biophysics, Chinese Academy of Sciences, China) for help in the retrovirus packaging experiments.

Funding

This work was supported by grants from the National HighTec Research Developing Programme (2006AA02A310) of China, the Special Funds for Major State Basic Research of China (2006CB910802), the National Natural Science Foundation of China for Innovation group (30621063), and the State Key Laboratory of Proteomics (SKLP-K200801).

References

1 Young J and Povey S. The genetic basis of tuberous sclerosis. Mol Med Today 1998, 4: 313–319.
2 van Slegtenhorst M, Nellist M, Nagelkerken B, Cheadle J, Snell R, van den Ouweland A and Reuser A, *et al*. Interaction between hamartin and tuberin, the TSC1 and TSC2 gene products. Hum Mol Genet 1998, 7: 1053–1057.
3 Nellist M, van Slegtenhorst MA, Goedbloed M, van den Ouweland AM, Halley DJ and van der Sluijs P. Characterization of the cytosolic tuberin-hamartin complex. Tuberin is a cytosolic chaperone for hamartin. J Biol Chem 1999, 274: 35647–35652.
4 Krymskaya VP. Tumour suppressors hamartin and tuberin: intracellular signalling. Cell Signal 2003, 15: 729–739.
5 Hengstschlager M, Rodman DM, Miloloza A, Hengstschlager-Ottnad E, Rosner M and Kubista M. Tuberous sclerosis gene products in proliferation control. Mutat Res 2001, 488: 233–239.
6 Nellist M, Burgers PC, van den Ouweland AM, Halley DJ and Luider TM. Phosphorylation and binding partner analysis of the TSC1-TSC2 complex. Biochem Biophys Res Commun 2005, 333: 818–826.
7 Ballif BA, Roux PP, Gerber SA, MacKeigan JP, Blenis J and Gygi SP. Quantitative phosphorylation profiling of the ERK/p90 ribosomal S6 kinase-signaling cassette and its targets, the tuberous sclerosis tumor suppressors. Proc Natl Acad Sci USA 2005, 102: 667–672.
8 Alberts B. The cell as a collection of protein machines: preparing the next generation of molecular biologists. Cell 1998, 92: 291–294.
9 Gavin AC and Superti-Furga G. Protein complexes and proteome organization from yeast to man. Curr Opin Chem Biol 2003, 7: 21–27.
10 Orimoto K, Tsuchiya H, Sakurai J, Nishizawa M and Hino O. Identification of cDNAs induced by the tumor suppressor Tsc2 gene using a conditional expression system in Tsc2 mutant (Eker) rat renal carcinoma cells. Biochem Biophys Res Commun 1998, 247: 728–733.
11 Sen B, Wolf DC and Hester SD. The transcriptional profile of the kidney in Tsc2 heterozygous mutant Long Evans (Eker) rats compared to wild-type. Mutat Res 2004, 549: 213–224.
12 Rosner M, Freilinger A, Lubec G and Hengstschlager M. The tuberous sclerosis genes, TSC1 and TSC2, trigger different gene expression responses. Int J Oncol 2005, 27: 1411–1424.
13 Rosner M, Hofer K, Kubista M and Hengstschlager M. Cell size regulation by the human TSC tumor suppressor proteins depends on PI3K and FKBP38. Oncogene 2003, 22: 4786–4798.

14 Hengstschlager M, Rosner M, Fountoulakis M and Lubec G. Regulation of PCNA and CAF-1 expression by the two tuberous sclerosis gene products. Biochem Biophys Res Commun 2003, 307: 737–742.
15 Hengstschlager M, Rosner M, Fountoulakis M and Lubec G. Tuberous sclerosis genes regulate cellular 14-3-3 protein levels. Biochem Biophys Res Commun 2003, 312: 676–683.
16 Hengstschlager M, Rosner M, Fountoulakis M, Oh JE and Lubec G. Protein levels of alpha1-tubulin, protein disulfide isomerase, tropomyosins and vimentin are regulated by the tuberous sclerosis gene products. Cancer Lett 2004, 210: 219–226.
17 Rigaut G, Shevchenko A, Rutz B, Wilm M, Mann M and Seraphin B. A generic protein purification method for protein complex characterization and proteome exploration. Nat Biotechnol 1999, 17: 1030–1032.
18 Puig O, Caspary F, Rigaut G, Rutz B, Bouveret E, Bragado-Nilsson E and Wilm M, *et al*. The tandem affinity purification (TAP) method: a general procedure of protein complex purification. Methods 2001, 24: 218–229.
19 Gingras AC, Aebersold R and Raught B. Advances in protein complex analysis using mass spectrometry. J Physiol 2005, 563: 11–21.
20 Gao G, Guo X and Goff SP. Inhibition of retroviral RNA production by ZAP, a CCCH-type zinc finger protein. Science 2002, 297: 1703–1706.
21 Jin WH, Dai J, Li SJ, Xia QC, Zou HF and Zeng R. Human plasma proteome analysis by multidimensional chromatography prefractionation and linear ion trap mass spectrometry identification. J Proteome Res 2005, 4: 613–619.
22 Yamamoto Y, Jones KA, Mak BC, Muehlenbachs A and Yeung RS. Multicompartmental distribution of the tuberous sclerosis gene products, hamartin and tuberin. Arch Biochem Biophys 2002, 404: 210–217.
23 Jansen FE, Notenboom RGE, Nellist M, Goedbloed MA, Halley DJ, de Graan PNE and van Nieuwenhuizen O. Differential localization of hamartin and tuberin and increased S6 phosphorylation in a tuber. Neurology 2004, 63: 1293–1295.
24 Fukuda T, Kobayashi T, Momose S, Yasui H and Hino O. Distribution of Tsc1 protein detected by immunohistochemistry in various normal rat tissues and the renal carcinomas of Eker rat: detection of limited colocalization with Tsc1 and Tsc2 gene products in vivo. Lab Invest 2000, 80: 1347–1359.
25 Burkhard P, Stetefeld J and Strelkov SV. Coiled coils: a highly versatile protein folding motif. Trends Cell Biol 2001, 11: 82–88.
26 Shirai A, Matsuyama A, Yashiroda Y, Hashimoto A, Kawamura Y, Arai R and Komatsu Y, *et al*. Global analysis of gel mobility of proteins and its use in target identification. J Biol Chem 2008, 283: 10745–10752.
27 Ahmad QR, Nguyen DH, Wingerd MA, Church GM and Steffen MA. Molecular weight assessment of proteins in total proteome profiles using 1D-PAGE and LC/MS/MS. Proteome Sci 2005, 3: 6.
28 Rosner M, Hanneder M, Siegel N, Valli A and Hengstschlager M. The tuberous sclerosis gene products hamartin and tuberin are multifunctional proteins with a wide spectrum of interacting partners. Mutat Res 2008, 658: 234–246.
29 Lieber MR, Ma Y, Pannicke U and Schwarz K. The mechanism of vertebrate nonhomologous DNA end joining and its role in V(D)J recombination. DNA Repair (Amst) 2004, 3: 817–826.
30 Meek K, Gupta S, Ramsden DA and Lees-Miller SP. The DNA-dependent protein kinase: the director at the end. Immunol Rev 2004, 200: 132–141.
31 Bladen CL, Udayakumar D, Takeda Y and Dynan WS. Identification of the polypyrimidine tract binding protein-associated splicing factor. p54(nrb) complex as a candidate DNA double-strand break rejoining factor. J Biol Chem 2005, 280: 5205–5210.
32 Soucek T, Holzl G, Bernaschek G and Hengstschlager M. A role of the tuberous sclerosis gene-2 product during neuronal differentiation. Oncogene 1998, 16: 2197–2204.
33 Tavazoie SF, Alvarez VA, Ridenour DA, Kwiatkowski DJ and Sabatini BL. Regulation of neuronal morphology and function by the tumor suppressors Tsc1 and Tsc2. Nat Neurosci 2005, 8: 1727–1734.